Available online at www.sciencedirect.com
ScienceDirect
European Journal of Medicinal Chemistry 43 (2008) 2479–2488
EUROPEAN JOURNAL OF MEDICINAL CHEMISTRY
http://www.elsevier.com/locate/ejmech

Original article

Identification of "toxicophoric" features for predicting drug-induced QT interval prolongation

Alessio Coi [a,1], Ilaria Massarelli [b,1], Lara Testai [c,1], Vincenzo Calderone [c], Anna Maria Bianucci [a,*]

[a] *Dipartimento di Scienze Farmaceutiche, Università di Pisa, Via Bonanno 6, 56126 Pisa, Italy*
[b] *Dipartimento di Chimica e Chimica Industriale, Università di Pisa, Via Risorgimento 35, 56126 Pisa, Italy*
[c] *Dipartimento di Psichiatria, Neurobiologia, Farmacologia e Biotecnologie, Università di Pisa, Via Bonanno 6, 56126 Pisa, Italy*

Received 20 June 2007; received in revised form 7 December 2007; accepted 11 December 2007
Available online 5 January 2008

Abstract

Drugs delaying cardiac repolarization by blockade of hERG K^+ channel generally prolong the QT interval of the electrocardiogram, an effect regarded as a cardiac risk factor with the potential to cause '*torsade des pointes*'-type arrhythmias in humans. The present study applied a homology building technique and molecular dynamics simulations to model the pore of hERG K^+ channel. A docking analysis was then performed on selected ligands which were classified as QT-prolonging or non-prolonging after experimental measurements in *in vivo* anesthetized guinea pig. The results of this structural analysis provided a "toxicophoric" model that was further exploited to inspect a dataset of known QT-prolonging/non-prolonging molecules. The emerging major chemical features to be avoided, in order to obtain cardiac safe therapeutic agents, comprise the simultaneous presence of (i) a protonated nitrogen atom within an observed range of distances from a heteroatom; (ii) aromatic groups capable of interacting within an area defined by Gly657 residues of the pore or within an area located at the top of the longitudinal axis of the pore. Moreover, additional hydrophobic moieties interacting with one of the equatorial cavities located in the area near-by Tyr652 residues and/or with a hydrophobic ring defined by Phe656 residues should be avoided.

Keywords: hERG K^+ channel; Toxicophore; QT interval prolongation; Molecular modeling; Homology building

1. Introduction

Several clinically used drugs produce undesired blockade of the cardiac hERG (human Ether-a-go-go Related Gene) K^+ channel, carrying the repolarizing current I_{Kr}. This effect results in prolongation of the cardiac monophasic action potential which, at the level of the electrocardiogram, manifests itself as a prolongation of the QT interval [1,2]. When this attains critical levels, depolarization signals can fall into the prolonged repolarization process, thereby favoring the generation of life-threatening polymorphic ventricular tachyarrhythmia, known as *torsade des pointes* (TdP), which can evolve into irreversible ventricular fibrillation.

The risk associated with the torsadogenic cardiotoxicity of QT interval prolonging drugs has been the subject of authoritative documents produced by International Conference on Harmonization, mandating adequate non-clinical and clinical evaluations of the cardiac safety of drug candidates [3]. Consequently, in the last decade, public and private research efforts have been routinely addressed to develop experimental strategies for early recognition of the effects of compounds on hERG K^+ channels and/or on the QT interval.

Among various preclinical experimental approaches, our group developed an *in vivo* experimental model. It enables the generation of data necessary to develop *in silico* models for correlating the cardiotoxic effects of recognized torsadogenic agents to their ability to prolong QT interval in

* Corresponding author. Tel.: +39 050 2219564.
E-mail address: bianucci@dcci.unipi.it (A.M. Bianucci).
[1] Authors equally contribute to the work.

0223-5234/$ - see front matter © 2007 Elsevier Masson SAS. All rights reserved.
doi:10.1016/j.ejmech.2007.12.025

anaesthetized guinea pigs [4]. This model [5] and/or *in vitro* isolated and perfused hearts from this animal [6] are sensitive and convenient experimental assays for detecting drugs with the propensity to cause pro-arrhythmic effects resulting from repolarization delay in humans.

Drugs blocking cardiac hERG channel belong to a variety of chemical, pharmacological, and therapeutic classes [7]. Therefore, they offer a real challenge for computational chemists attempting to identify suitable ''toxicophoric'' models allowing correlating the unwanted biological effect with the structural and chemical features.

In a previous work, we reviewed experimental and clinical reports on torsadogenic properties of antipsychotic drugs, by using a simple Molecular Mechanic (MM) approach to identify common structural elements shared by these drugs and accounting for their torsadogenic properties [8]. A more recent work from our laboratory presented a ligand-based approach consisting of a QSAR study of a series of molecules for which published patch clamp IC_{50} values were available. The predictive ability of the model was validated by applying rigorous criteria to a blind set of molecules (disjoined from the whole dataset initially considered) employing highly diagnostic statistical parameters [9].

In the present paper, the QT interval effects of 18 drugs (Fig. 1) were determined in anaesthetized guinea pigs. Thirteen of these molecules were selected because they share

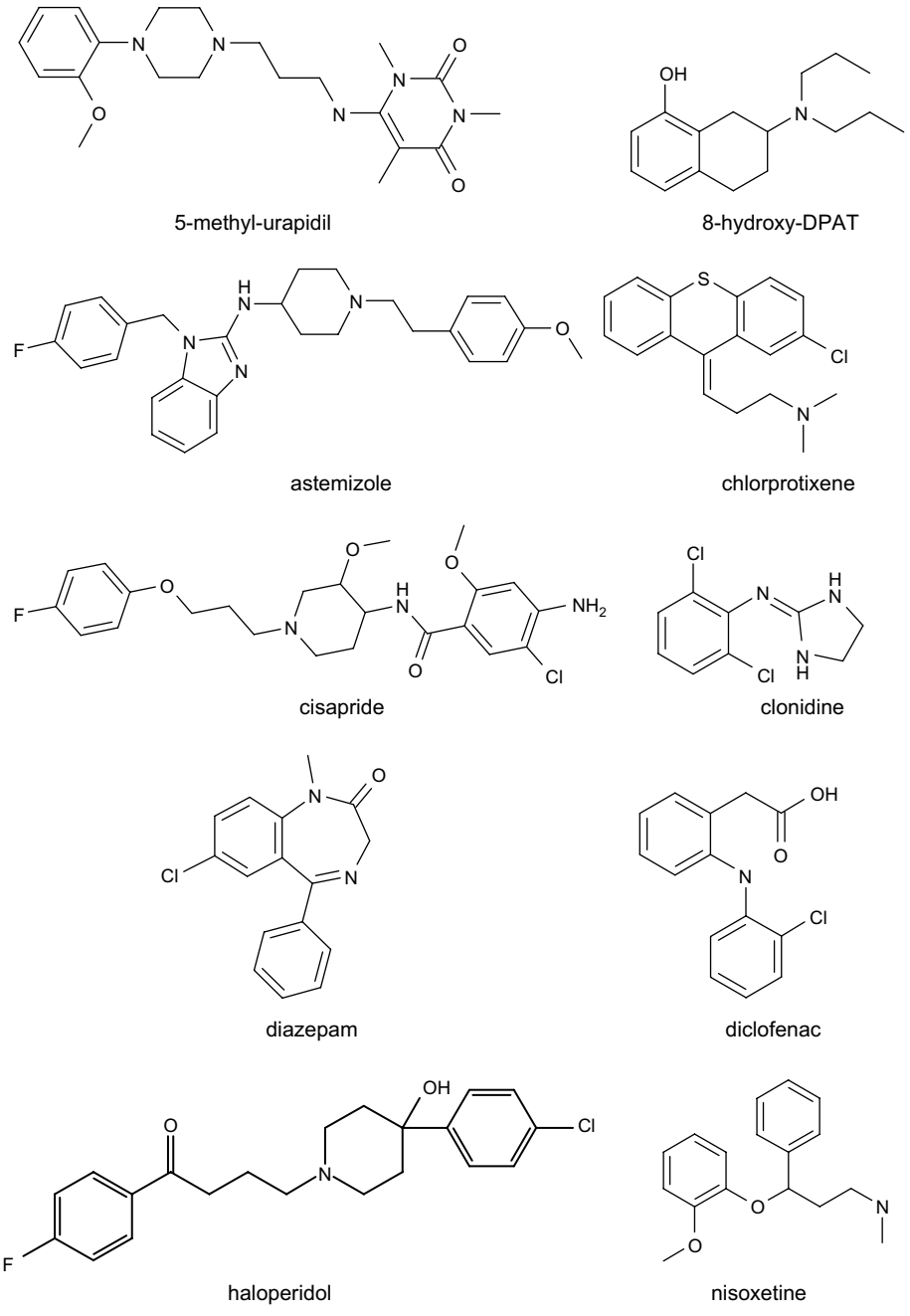

Fig. 1. The 18 selected drus, investigated for their QT-prolonging effect.

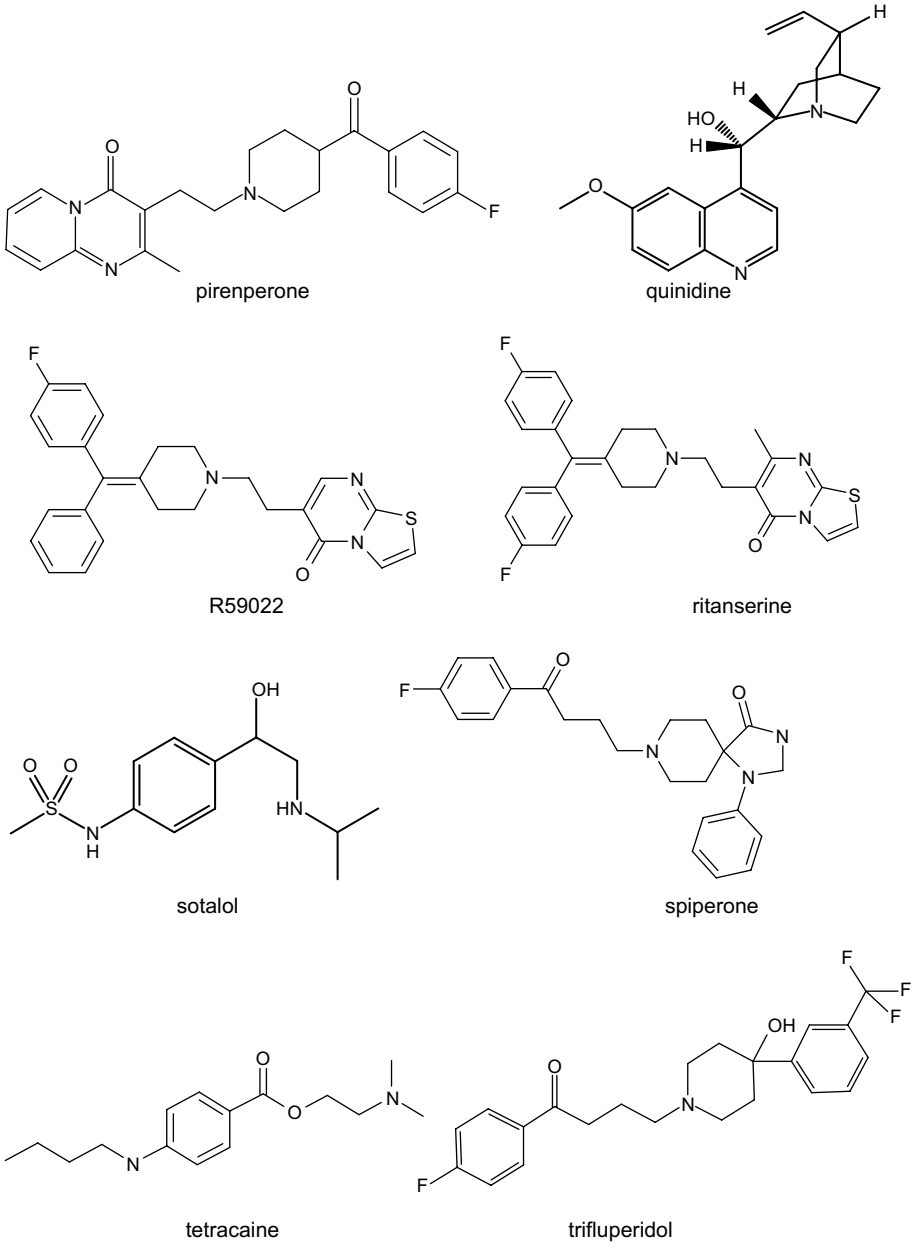

Fig. 1. (*continued*).

common structural characteristics, identified in our previous model as minimal requirements for a drug to be torsadogenic [8]. The remaining five molecules (clonidine, chlorprotixene, diazepam, diclofenac, and 5-methyl-urapidil) were selected as ''negative control''. Within the sub-group of 13 compounds, five molecules (astemizole, haloperidol, quinidine, cisapride, sotalol) are recognized to be torsadogenic drugs in humans whereas eight molecules have not been previously studied for this property.

In this work, a theoretical model of the 3D structure of the channel pore was constructed by homology modeling. Computational techniques that exploit molecular dynamics (MD) simulations and a subsequent molecular docking of the selected drugs into the pore lumen, allowed drawing a probabilistic ''toxicophoric'' model satisfactorily accounting for chemical and spatial features responsible for drug-induced QT interval prolongation.

2. Results and discussion

2.1. Torsadogenic cardiotoxicity

The list of drugs investigated for their QT-prolonging effect, with the corresponding potency index (pEC_{50} representing the dose in g/kg of the compounds expressed as −log evocking a QTcB interval prolongation of 50 ms) is reported in Tables 1 and 2. Well-established torsadogenic drugs (astemizole, cisapride, haloperidol, quinidine, and sotalol) produced the expected dose-dependent QTcB-prolongation with respect to baseline QTcB value. Moreover, 8-hydroxy-DPAT,

Table 1
List of known QT-prolonging molecules with $pEC_{50\ ms}$ values expressed as −log of the drug dose (g/kg) ± SEM and E_{max} ± SEM (ms)

Compounds	$pEC_{50\ ms}$ ± SEM	E_{max} ± SEM
Astemizole	3.74 ± 0.11	111.3 ± 10.9
Cisapride	3.00 ± 0.086	81.9 ± 14.2
Haloperidol	3.48 ± 0.13	123.3 ± 19.9
Quinidine	2.55 ± 0.077	78.6 ± 12.9
Sotalol	2.77 ± 0.053	97.3 ± 26.8

R59022, ritanserine, spiperone, tetracaine and trifluperidol, previously not studied in the anesthetized guinea pig model, were also found to prolong the QTcB interval. Such a finding confirms the good predictive ability of our previous pharmacophoric model [8], although these drugs are considered to be cardiac safe in humans since no published report on this subject is available to our knowledge (Table 2). Only two of the above compounds did not satisfy the model prediction: these are pirenperone which decreased the QT interval duration, and nisoxetine which prolonged the QT interval at the highest investigated dose (10.0 mg/kg).

The negative control-drugs (chlorprotixene, clonidine, diazepam, diclofenac and 5-methyl-urapidil) did not produce significant QT interval changes (Table 2).

Among the drugs that were found to prolong the QT interval, ritanserine and R59022, at the dose of 10.0 mg/kg also caused marked bradyarrhythmia and death, before the highest dose programmed (10 mg/kg, i.v.) could be investigated. The lethal effect may result from cardiac depression mediated by blockade of cardiac and vascular Ca^{2+} channels. In a group of animals, the vehicles used were shown not to produce significant changes on QTcB interval (data not shown). All the above results were exploited for obtaining the new ''toxicophoric'' model presented here.

Table 2
List of other assayed compounds expected to possess or not to possess QT-prolonging properties with $pEC_{50\ ms}$ values expressed as −log of the drug dose (g/kg) ± SEM and E_{max} ± SEM (ms)

Compounds	$pEC_{50\ ms}$ ± SEM	E_{max} ± SEM
Clonidine	–	–
Chlorprotixene	–	–
Diazepam	–	–
Diclofenac	–	–
5-Methyl-urapidil	–	–
Nisoxetine[a]	–	37.5 ± 11.0
Pirenperone[b]	–	−116.0 ± 0.1
8-Hydroxy-DPAT	2.95 ± 0.064	116.3 ± 13.2
R59022[c]	3.24 ± 0.079	79.5 ± 1.0
Ritanserine[c]	4.05 ± 0.075	106.8 ± 26.0
Spiperone	2.99 ± 0.086	100.0 ± 21.5
Tetracaine	2.62 ± 0.089	91.5 ± 8.5
Trifluperidol	2.51 ± 0.13	74.7 ± 25.3

[a] $EC_{50\ ms}$ has not been calculated, since the E_{max} was lower than 50 ms.
[b] $EC_{50\ ms}$ has not been calculated, since this compound decreased QTc.
[c] The highest dose assayed was 3.0 mg/kg i.v. because of the lethal effect of the 10.0 mg/kg i.v. dose.

2.2. Homology building of the theoretical model and molecular docking

The 3D structure of the hERG K^+ channel is not yet available from directly gathered experimental data. For this reason, pore–ligand interactions were investigated by means of computational studies carried out on a homologous 3D model of the pore built from the crystal structure of a bacterial K^+ channel, as described in Section 4.

The debate on which state of the hERG channel the blockers bind to is still open. Mitcheson et al. used the KcsA template enabling to represent the channel in its closed state and performed alanine-scanning mutagenesis and homology modeling to determine the structural basis for drugs blocking the hERG channel [10]. Other authors, such as Sanchez-Chapula et al. [11], Moreno et al. [12], Frenal et al. [13], and Perry et al. [14,15], also modeled the closed state of the hERG channel with the purpose of a subsequent molecular docking study. On the other hand, Pearlstein et al. and Choe et al. used the structure of MthK and KvAP respectively, resembling the open state of the channel [16,17]. Rajamani et al. developed homology models based on available K^+ channel structures, constructing representations resembling an open and a partially open state of the channel. Models derived for the open or partially open states exclusively resulted in very poor fit, so they grouped the ligands into bins based on their preference for a particular state of the channel to overcome this problem [18].

It is known from electrophysiology experiments that the channel must be in the active open state in order to bind many ligands. In this condition, the cavity residues, suggested to play a relevant role for binding in mutation studies, are accessible. However, once a compound enters the cavity region, the S6 helices can close at different amounts, depending on the ligand bound. On the basis of these observations, we chose to inspect the interactions between the selected drugs and the closed state of the channel.

Since the binding most likely involves interactions with the inner walls of the channel pore, the orientation of backbone and side chain groups lining the pore is of great relevance for interaction with drugs. Hence, the side chains of Tyr652 and Phe656, for example, were of particular interest for such interactions.

The 3D model of the pore was subjected to MD simulations as described in Section 4 and the optimized structure was then used as the molecular target for docking all the selected ligands.

The lumen of the modeled pore consists of two layers of aromatic side chains containing Phe656 and Tyr652 (chains A–D). The proposed binding mode of ligands docked in the pore is in agreement with literature data, concerning residues involved in the pharmacological interaction between drugs and the pore itself. The Phe656 side chains appear to be of particular relevance for binding, since they define a rather narrow ring that engages π-stacking interactions with hydrophobic regions of the ligands. Tyr652 is proposed to allow a π-cation interaction with the basic nitrogen of most ligands. The pore

presents a rather polar environment with several potentially favorable interactions close to the selectivity filter. The side chains of Thr623, Ser624, and Val625 can interact with polar groups present in some ligand moieties.

2.3. Structure-based analysis of ligand–pore interactions and ''toxicophore'' generation

Molecules of Fig. 1 show a relevant structural diversity that makes the identification of a commonly shared ''toxicophore'' very challenging. A molecular docking-based approach was exploited as an attempt to overcome such a difficulty.

The starting orientations of the longitudinal axes of all the molecules were set along the pore axis, so that the hydrophobic moieties of the ligands are located at the intracellular mouth site and their tail regions point toward the selectivity loop of the pore.

The molecular docking process generated clusters of different configurations for each ligand within the pore cavity. The analysis of the lowest-energy configurations of each ligand–pore complex allowed identifying several locations within the binding site (Fig. 2). Ser624 residues (chains A–D) define a location, conventionally named ''**E**'', next to the extracellular opening of the pore, whereas, on the other side, Gly657 residues (chains A–D) define the ''**I**'' location, next to the intracellular opening of the pore. Hydrophobic complementarities were found in the region around Phe656 residues (chains A–D) which define a rather narrow ring, conventionally named the ''**H**'' location. Furthermore, four equatorial cavities ''**C**'' can be identified and result to be located in the area around Tyr652. This residue in particular can act as a π-cation interaction site with a positively charged group, the protonated basic nitrogen (**N**), of the ligand. A (**Z**) hetero-atom of the ligand itself (a H-bond acceptor) located at a ranged distance [8] from (**N**) can interact with one of the equatorial locations defined by residues Tyr652, Ala653, Phe656.

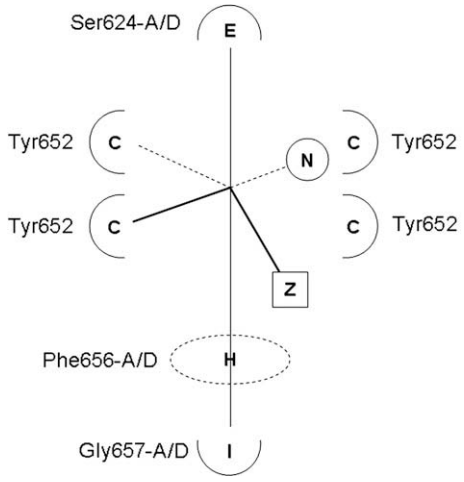

Fig. 2. Binding locations: **E**, **C** (''equatorial'' cavities), **H** (hydrophobic pocket), and **I**. (**N**) and (**Z**) are the basic nitrogen and a hetero-atom of the ligand, respectively.

The structure of astemizole was chosen as the staring point for identifying possible ''toxicophoric'' features, since this molecule is one of the most potent QT interval prolonging drugs in our assay (Table 1).

Interactions of astemizole and ritanserine with the pore appear to involve the basic nitrogen of the piperidine ring (**N**). The coordinates of the centers of mass of the two close aromatic moieties suggest that they fit, respectively, into **E** and **C** locations of the pore (Fig. 3). Moreover a second aromatic group is capable of engaging π-stacking interactions with Phe656 side chains at the **H** location. Moreover, with respect to the biologically active conformation of the ligands, a (**Z**) hetero-atom (oxygen atom of the carbonilic group in ritanserine and the non-substituted N atom of the benzimidazole ring in astemizole) is placed at a 5.01 and 6.07 Å distance from (**N**) in ritanserine and astemizole, respectively. A subsequent detailed analysis indicates that (**Z**) and/or an (**N**)–(**Z**) distance comprised within a specific range and mentioned in Ref. [8], appear to act as potency-modulating features.

The analysis of the other selected ligands was subsequently performed to identify a set of minimal and common requirements for the QT-prolonging activity. Hence, $EC_{50\ ms}$ values expressed in g/kg (Tables 1 and 2) were converted into μmol/kg in order to compare the potency of the considered ligands according to their binding mode (Table 3). This allowed ranking molecules into three groups on the basis of their potency: (1) astemizole, haloperidol, ritanserine, and R59022 ($EC_{50\ ms}$ <1.28 μmol/kg); (2) cisapride, spiperone, and 8-hydroxy-DPAT (2.12 μmol/kg < $EC_{50\ ms}$ < 4.58 μmol/kg); and (3) sotalol, quinidine, trifluperidol, and tetracaine ($EC_{50\ ms}$ >6.20 μmol/kg).

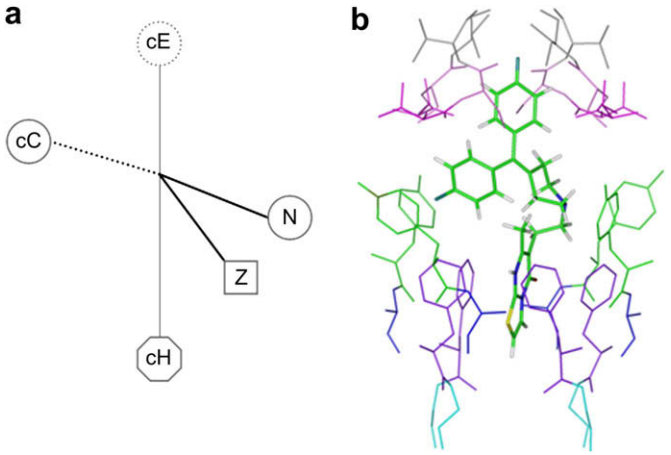

Fig. 3. a) Critical features in the binding site for ritanserine and astemizole. cE, cC, and cH are the aromatic groups interacting at **E**, **C** and **H** locations, respectively. (b) Stereoview of ritanserine docked in the pore binding pocket. Residues Thr623, Ser624, Val625, Tyr652, Ala653, Phe656 and Gly657 are respectively colored in magenta, pink, grey, green, blue, violet and light blue. The **E** location is at the top (Thr623, Ser624, Val625). The (**N**) and (**Z**) atoms of ritanserine are colored by atom type. The interacting locations **C** (on the left) and **H** are colored in green and violet, respectively. The remaining ''equatorial'' cavities (on the right and at the center of the view) are also colored in green (for interpretation of the references to color in this figure legend, the reader is referred to the web version of this article).

Table 3
List of blockers as resulted from QT-prolongation measurement with $EC_{50\ ms}$ expressed as μmol/kg

Compounds	$EC_{50\ ms}$ (μmol/kg)
Ritanserine	0.19
Astemizole	0.39
Haloperidol	0.88
R59022	1.28
Cisapride	2.12
Spiperone	2.55
8-Hydroxy-DPAT	4.57
Sotalol	6.20
Quinidine	8.34
Trifluperidol	7.65
Tetracaine	9.04

Haloperidol, spiperone and trifluperidol have the (**N**) and (**Z**) groups, moreover they present two aromatic moieties which interact with the **I** and **E** locations of the pore (Fig. 4a and d for the docked conformation of haloperidol). Centroids were defined for the aromatic rings of these three ligands and the distances between the two centroids, between the centroids and the **N** atom, and between **N** and **Z** appear to modulate their relative potency (Table 4). Hence, increasing the **cI**−**cE** distance and decreasing the **N**−**Z** distance lowers the activity in this group of molecules. Finally, the occupancy of the **I** location seems to balance the absence of structural elements interacting at the equatorial **C** location, as previously seen for the case of ritanserine and astemizole.

Fig. 4b shows that the binding features of blocker R59022 are similar to the ones presented by haloperidol, spiperone and trifluperidol. A further interaction point at a second cavity **C** is found which, however, does not seem to enhance its activity in comparison to haloperidol. In Fig. 4e is also reported the conformation of R59022 docked in the pore.

Cisapride assumes the same space orientation as ritanserine and astemizole, but in addition it interacts with a second equatorial **C** location. However, some geometric parameters may explain its reduced activity, since **cE**−**cC**, **cE**−**cH**, **cE**−**N**, **cC**−**N** distances are significantly lower than the ones reported for ritanserine and astemizole (Table 5). The molecular shape

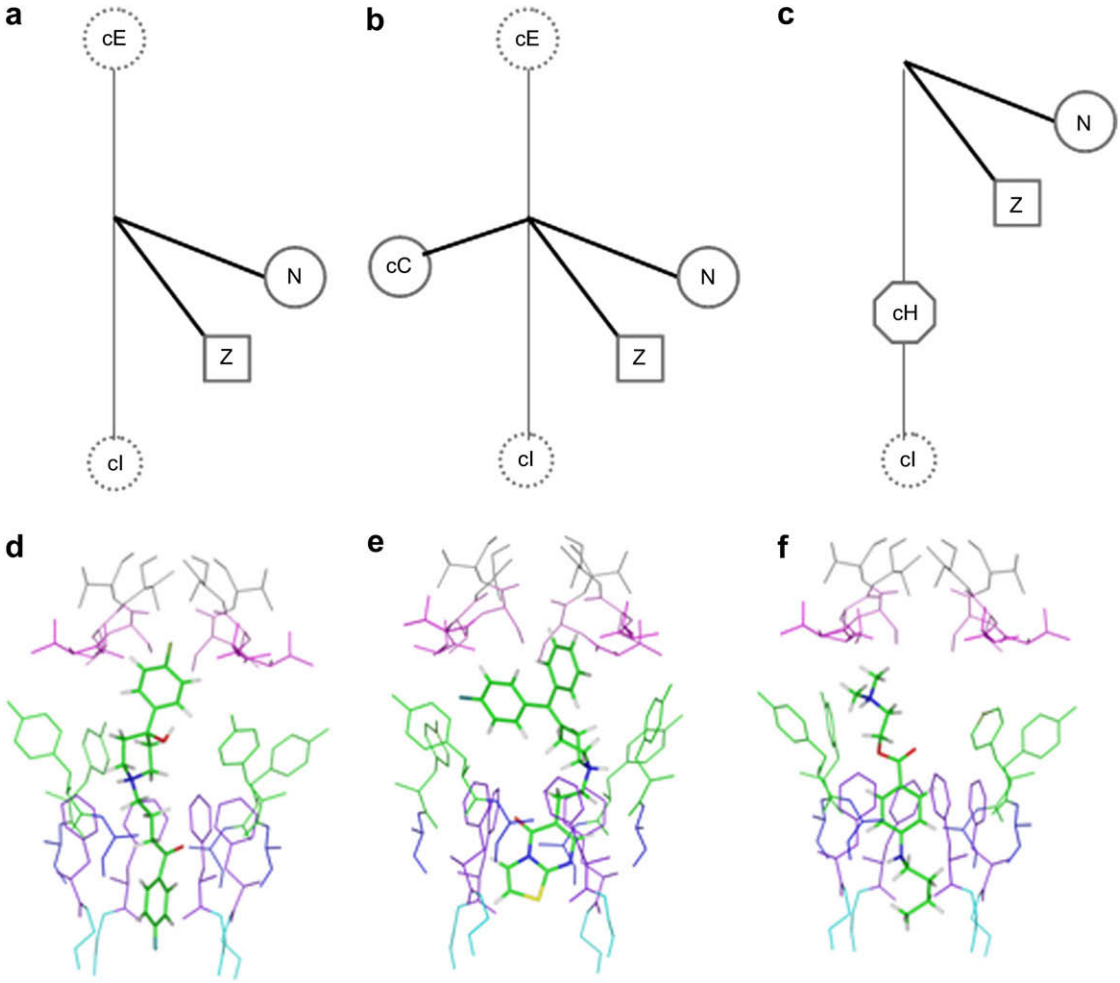

Fig. 4. Binding features for (a) haloperidol, spiperone, trifluperidol, (b) R59022, (c) tetracaine, sotalol. cE, cC, cH, and cI are the aromatic groups interacting at **E**, **C**, **H** and **I** locations, respectively. In the figure, the conformation docked in the pore of a representative ligand of the three sub-groups is also reported: (d) haloperidol, (e) R59022 and (f) tetracaine. Residues Thr623, Ser624, Val625, Tyr652, Ala653, Phe656 and Gly657 are respectively colored in magenta, pink, grey, green, blue, violet and light blue (for interpretation of the references to color in this figure legend, the reader is referred to the web version of this article).

Table 4
Geometric parameters determined for haloperidol, spiperone and trifluperidol

Compounds	**cI**–**cE** (Å)	**N**–**Z** (Å)
Haloperidol	12.81	5.24
Spiperone	12.97	5.22
Trifluperidol	13.25	5.03

cI and **cE** are the centroids for the aromatic rings interacting at the **I** and **E** locations, respectively.

of cisapride is shorter and larger than those of the most potent QT-prolonging molecules of the dataset, suggesting that the major critical feature involved in the modulation of the activity could relay in an ''ideal'' molecular length.

Tetracaine and both sotalol enantiomers are the only QT-prolonging molecules that do not interact with the **E** location (Fig. 4c and f for the docked conformation of tetracaine), although they establish hydrophobic interactions at **H** and **I**. However, they belong to the sub-group of drugs with weakest potency. Hence, interactions at the **E** location, already observed among the ones established by ritanserine and astemizole, appear to be a relevant, but not an essential requirement for the torsadogenic activity.

As far as molecules not showing QT-prolongation are concerned, the following conclusion may be drawn, with regard to the pore region binding locations: pirenperone, chlorprotixene and nisoxetine have no anchor points at **I** and **E** areas. Otherwise, diazepam, diclofenac and clonidine have no (**N**) atom in their chemical structure.

The detailed analysis described above allowed defining a minimal set of molecular features for a new ''toxicophore'' accounting for QT-prolonging activity.

The major chemical features to be avoided in order to obtain cardiac safe therapeutic agents comprise the simultaneous presence of

(i) the (**N**) and (**Z**) atoms within an observed range of distances;
(ii) aromatic groups capable of interacting at **I** or **E** locations,

where the **E** interaction area is located at the top of the longitudinal axis of the pore, close to residues Ser624 (A–D chains), while the **I** location involves Gly657 residues (A–D chains). Moreover, additional hydrophobic moieties which could interact with **C** and/or **H** locations should be avoided. The **H** location is a rather narrow ring defined by Phe656 residues of the four A–D chains. Finally, the **C** locations represent the four equatorial cavities located in the area near-by Tyr652 residues. With regard to the ligand characteristics, (**N**) represents the protonated nitrogen atom facing Tyr652, while the hetero-atom (**Z**), located at optimal distance from (**N**) and laying near Tyr652 and Ala653, usually acts as H-bond acceptor. Hence, the optimal (**N**)–(**Z**) distance for interaction, is approximately 4.5 Å long as already indicated in our previous work [8].

Table 5
Geometric parameters determined for ritanserine, astemizole and cisapride

Compounds	**cE**–**cC** (Å)	**cE**–**cH** (Å)	**cE**–**N** (Å)	**cC**–**N** (Å)
Ritanserine	4.98	10.57	6.45	6.42
Astemizole	4.77	12.43	7.29	5.89
Cisapride	3.56	9.63	3.84	5.08

cE, **cC** and **cH** are the centroids for the rings interacting at the **E**, **C**, and **H** locations, respectively.

After that, in order to evaluate the qualitative prediction ability of the ''toxicophore'', 18 representative known QT-prolonging/non-prolonging and, at the same time, hERG blocking/non-blocking molecules (Table 6) were selected and analyzed taking into account the previously described chemical and structural requirements for QT interval prolongation. The molecules were docked into the binding site of the 3D theoretical model of the hERG pore; for each ligand, orientations and conformations optimized by molecular docking in the pore cavity were considered for the structural analysis. All the molecules showed final orientations in accordance with our hypotheses; in particular, the eight known QT-prolonging (and hERG blocking) compounds possess the characteristics hypothesized for conferring QT-prolonging activity. On the other hand the non-prolonging (and non-blocking) compounds either lack the (**N**) atom or do not show interactions at the **I** or **E** locations. These observations strongly support the discriminating ability of the ''toxicophoric'' model proposed here.

The ''toxicophore'' derived from this structure-based investigation relies on specific spatial occupancy that leads to the identification of binding locations within the pore region. In the recent years, different ligand-based pharmacophores were proposed by some authors who obtained good results even if they did not exploit the 3D structure of the hERG pore. Ekins et. al. proposed a pharmacophore model based on the Catalyst program [23]. Such a model is defined by four hydrophobic and one positively ionizable sites, located at reciprocally well-defined distances. It was obtained by a ligand-based approach and takes into account, for each inhibitor, plausible conformers generated by the program, disregarding molecular docking at the pore region.

Cavalli et al. described a CoMFA-derived pharmacophore consisting of three aromatic moieties connected through a nitrogen function (tertiary amine) which are geometrically described by ranges of distances and angles between the four points of the pharmacophore that was also generated only from ligand-based information [41].

Similarly, our early work exploited ligand-based information to derive a simple pharmacophoric model comprising a basic, sterically hindered nitrogen atom and a moiety capable of acting as a hydrogen-bond acceptor with the specific range distance between these two sites [8].

In 2004, Aronov and Goldman proposed another ligand-based three-binding point-pharmacophore consisting of a hydrogen-bond acceptor located between positively charged nitrogen and an aromatic ring [42].

Therefore, the ''toxicophoric'' model presented here could give further suggestions, defining some features commonly

Table 6
Dataset of known QT-prolonging/non-prolonging molecules contemporarily selected according to their strong hERG blocking/non-blocking activity

Compound	pIC_{50}	Reference	Compound	pIC_{50}	Reference
Desmethylastemizole	3.00	[19]	Lignocaine	−2.42	[35]
Pimozide	2.52	[20,21]	Nicotine	−2.39	[23]
MK499	1.67	[22]	Lamotrigine	−2.36	[36]
E-4031	1.64	[21,23–28]	Methylecgonidine	−2.23	[37]
Norastemizole	1.56	[19]	Tadalafil	−2.00	[38]
Droperidol	1.49	[29]	Meperidine	−1.88	[39]
Dofetilide	1.31	[26,30–32]	Pilsicainide	−1.31	[40]
Domperidone	1.24	[33]	Desmethylolanzapine	−1.15	[23]
Phenobarbital	−3.48	[34]	2-Hydroxy-methyl olanzapine	−1.06	[23]

pIC50 (−log IC50 expressed as μM) values are also reported. IC50 were averaged over data about the same molecule coming from different experiments all referring to HEK cells.

shared by known QT-prolonging molecules, and describing specific spatial occupancy of various potentially binding areas, identified with the aid of a theoretical 3D model of the pore.

3. Conclusions

A ''toxicophore'' for QT-prolonging drugs was obtained after exploring interactions between QT-prolonging and non-prolonging molecules and a theoretical 3D model of the hERG channel pore, obtained from a homologous K^+ channel protein. Molecular dynamics simulations and a subsequent molecular docking procedure were applied to achieve a satisfactory description of the ''toxicophore''. Thus, the use of a 3D model of the pore and the availability of a number of meaningful ligands allowed identifying some major interaction areas. The residues playing the most significant roles for such interactions are Tyr652, Phe656 and Thr623, Ser624, Val625. Phe656 is involved in a π-stacking interaction with the hydrophobic moieties of the ligands, whereas Tyr652 is proposed to undergo a π-cation interaction with a basic protonated nitrogen.

Residues Thr623, Ser624 and Val625 are capable of interacting with polar groups of some inhibitors. Docking the molecules of the analyzed set into the model led to discover preferential binding modes of different ligands within the pore, thus allowing accurate identification of peculiar molecular features and spatial arrangement required for conferring QT-prolonging (or non-prolonging) activity. The results obtained from the structural analysis of the complexes globally allowed an exhaustive description of the molecular features that give rise to the proposed ''toxicophoric'' model.

The major chemical features to be avoided, in order to obtain cardiac safe therapeutic agents, comprise the simultaneous presence of (i) a protonated nitrogen atom (**N**) within an observed range of distances from a heteroatom (**Z**); (ii) aromatic groups capable of interacting within an area (**I** location) defined by Gly657 residues of the four A–D chains or within an area (**E** location) located at the top of the longitudinal axis of the pore, close to residues Ser624 of the four A–D chains. Moreover, additional hydrophobic moieties which could interact with one of the four equatorial cavities (**C**) located in the area around Tyr652 residues and/or with the narrow ring defined by Phe656 residues (**H** location) should be avoided.

Then, the ''toxicophoric'' model generated by using *in vivo* data was exploited in order to inspect a dataset of selected molecules and revealed a good ability to assess the QT-prolonging profile.

In conclusion, the use of the proposed theoretical 3D model complemented by molecular docking procedures allows a useful *in silico* qualitative screening of newly designed molecules for early identification of drug candidates with potential QT-prolonging ability, which suggests to discard them for further development.

4. Experimental methods

4.1. Pharmacology

The experimental procedures were carried out in accordance with the Italian guidelines (D.L. 27/01/1992, no. 116) and European Community Council Directive 86/609 concerning care and use of laboratory animals.

The experimental procedure applied in this investigation has been previously described [4]. Briefly, male Dunkin-Hartley guinea pigs (400–500 g) were anaesthetized with sodium pentobarbital (60 mg/kg i.p., Sessa), the trachea cannulated and connected to a rodent ventilator pump (Basile mod. 7025), set to deliver 1 ml air/100 g of body weight at 70 strokes/min. The jugular vein was catheterized for intravenous injections.

Four electrodes were inserted subcutaneously in fore- and hind-limbs for recording Lead II and III of electrocardiogram (ECG) (Battaglia Rangoni electrocardiograph, MOD. AO/FC) and then connected to a polygraph (Battaglia Rangoni, MOD. KV380).

A 10-min stabilization time was allowed before initiating the intravenous injection of cumulative increasing (by a 3-fold factor) doses of each drug. The dose range of all test drugs was 0.1–10.0 mg/kg, with the exception of ritanserine and R59022, that were assayed in the range of 0.1–3.0 mg/kg, since the dose of 10 mg/kg showed a lethal effect.

A 20-min follow-up time was observed after each dose injection. Three ECG sequences of 10 s were recorded at the end of the follow-up period.

The administration of the highest dose of astemizole, cisapride, clonidine, chlorprotixene, haloperidol, 5-methyl-urapidil, pirenperone, sotalol, spiperone, and trifluperidol, requiring a volume of 4–5 ml of solution, was infused i.v. by Harvard Apparatus (MOD. 2400-001) at the rate of 0.4–0.5 ml/min, to avoid any significant influence of rapid changes of blood volume and/or plasmatic concentration of electrolytes.

All compounds were purchased from Sigma–Aldrich.

4.1.1. Data analysis

For each electrocardiographic recording RR and QT intervals were measured, and the QT correct (QTc) was calculated for heart rate by applying Bazett algorithm ($QTcB = QT/(RR)^{1/2}$). In this experimental procedure, the alternative QTc value calculated by applying Frediricia algorithm ($QTcF = QT/(RR)^{1/3}$) was not carried out since in a previous investigation we demonstrated virtually equivalent results by applying the two correction formulae [4].

For each dose, the maximal increase of the QTcB value, obtained at the end of the 20 min following the injection of the drug, was calculated. Data are reported as means ± S.E.M. of 5–6 experiments. Drug effects on cardiac repolarization are considered significant ($P \leq 0.05$) if the value of QTcB recorded in basal conditions (before the drug administration) or after the administration of a test drug are statistically different (Student *t*-test for unpaired data).

These experimental values were fitted with a sigmoid nonlinear regression algorithm (computer program: Graph Pad Prism 4.00), in order to calculate the potency index $pEC_{50\ ms}$, representing the dose in g/kg of the compound (expressed as −log) evoking a QTcB interval prolongation of 50 ms. These values as well as the efficacy parameter E_{max} (maximal QTcB increase produced by the highest dose of the drug injected) are also reported (Tables 1 and 2). In order to prevent the influence of the molecular weight of the compounds, the $pEC_{50\ ms}$, values were transformed also into the corresponding $EC_{50\ ms}$, representing the dose in μmol/kg evoking a 50 ms QTcB-prolongation.

4.2. Molecular modeling

The molecular modeling studies were mostly carried out by means of software running on an SGI Octane R12000 workstation.

The pore–ligand interactions were investigated by means of computational studies carried out on a homologous 3D model of the pore built from the crystal structure of a bacterial K^+ channel [*Streptomyces lividans* (1J95)] by using sequence alignment proposed Doyle et al. [43] (Fig. 5). Such a model gave rise to a pore region with a selectivity loop comprising four helices (tetramer) from the KcSA channel template.

The modeled hERG pore was then subjected to Molecular Dynamic (MD) simulations by using AMBER8.0 program in order to find low energy conformations [44]. Standard PARM99 force field parameters were assigned to the pore,

```
      61                                                    118
      |                                                      |
kcsa  TYPRALWWSVETATTVGYGDLYPVTLWGRLVAVVVMVAGITSFGLVTAALATWFVGRE
herg  KYVTALYFTFSSLTSVGFGNVSPNTNSEKIFSICVMLIGSLMYASIFGNVSAIIQRLY
      .*  **:::..: *:**:*:: * *   ::.:: **: *   :. : . ::: :
      |                                                      |
     610                                                    667
```

Fig. 5. Sequence alignment between Kcsa (P0A334) and hERG K^+ channel subunit (Q12809) used for homology based modeling of the pore.

using the LEAP program in AMBER8.0. A two-stage conjugate gradient energy minimization protocol was applied in order to avoid bad contacts prior to the MD simulations. A preliminary step of energy minimization was performed, where only the heavy atoms were restrained by using a harmonic potential of 1000.0 kcal/mol Å^2. Subsequently, restrained minimization was performed by using a much weaker force constant of 5.0 kcal/mol Å^2, where only the main-chain atoms were restrained. Both minimizations employed a distance dependent dielectric constant ($4r$) until a convergence tolerance drms $= 1.0 \times 10^{-3}$ kcal/mol Å was reached. After the minimization steps, MD simulations were started without explicit water, by using the pairwise Generalized-Born (GB) continuum solvent model of Hawkins and coworkers implemented in the SANDER module of AMBER8 [45,46]. No cut-off was applied during GB-MD simulations. Simulations employed 1 fs time step for 40,000 steps corresponding to a total of 40 ps of GB-MD. The final desired temperature of 298 K was obtained by requesting a heating cycle from 0 to 298 K over the course of the first 5000 MD steps and the Langevin dynamics were used to simulate solvent frictional effects with a collision frequency $\gamma = 1.0\ ps^{-1}$. Main-chain atoms were lightly restrained using a weak harmonic force constant of 5.0 kcal/mol Å^2, and the SHAKE algorithm was applied to constrain bonds involving hydrogen atoms [47]. The lowest-energy conformation of the pore was selected among the last 20 ps of the MD trajectory. The selected frame was further energy minimized with the same protocol described above, based on two-stage conjugate gradient energy minimization.

The 3D theoretical model of the hERG K^+ channel obtained after MD simulation was used for molecular docking studies. The structures of the molecules shown in Fig. 1 were built using the InsightII package [48] and considered in the protonated form of their basic nitrogen, where possible.

Each ligand was automatically docked into the pore model of the hERG K^+ using the DOCK5.2 program [49]. This approach allowed the identification of the most favorable orientation and conformation of each flexible ligand. DOCK5.2 allows docking flexible ligands into the active receptor site [48]. The program does not require generating a large number of conformations for the ligand, as the conformational space can be sampled by DOCK provided that the geometry of the initial ligand conformation is satisfactory.

Acknowledgment

The research described here was supported by the Italian Ministry of University and Research (MIUR) and by ISDD

S.r.l. (Via Marcora 11, Milano, Italy). Part of the calculations was performed at the CINECA computer facilities (Bologna, Italy).

References

[1] I. Cavero, M. Mestre, J.M. Guillon, W. Crumb, Expert Opin. Pharmacother. 1 (2000) 947–973.
[2] J.I. Vandenberg, B.D. Walker, T.J. Campbell, Trends Pharmacol. Sci. 22 (2001) 240–246.
[3] Committee for Proprietary Medicinal Products (CPMP), Points to Consider: The Assessment of the Potential for QT Interval Prolongation by Non-cardiovascular Medicinal Products, CPMP/986/96, 1997.
[4] L. Testai, V. Calderone, A. Salvadori, M.C. Breschi, P. Nieri, E. Martinotti, J. Appl. Toxicol. 24 (2004) 217–222.
[5] A. Takahara, A. Sugiyama, K. Hashimoto, Br. J. Pharmacol. 146 (2005) 561–567.
[6] H.C. Cheng, J. Incardona, B. McCullough, J. Pharmacol, Toxicol. Methods 54 (3) (2006) 278–287.
[7] A.M. Aronov, Drug Discov. Today 10 (2005) 149–155.
[8] L. Testai, A.M. Bianucci, I. Massarelli, M.C. Breschi, E. Martinotti, V. Calderone, Curr. Med. Chem. 11 (2004) 763–771.
[9] A. Coi, I. Massarelli, L. Murgia, M. Saraceno, V. Calderone, A.M. Bianucci, Bioorg. Med. Chem. 14 (2006) 3153–3159.
[10] J.S. Mitcheson, J. Chen, M. Lin, C. Culberson, M.C. Sanguinetti, Proc. Natl. Acad. Sci. U.S.A. 97 (2000) 12329.
[11] J.A. Sanchez-Chapula, R.A. Navarro-Polanco, C. Culberson, J. Chen, M.C. Sanguinetti, J. Biol. Chem. 277 (2002) 23587–23595.
[12] I. Moreno, R. Caballero, T. Gonzalez, C. Arias, C. Valenzuela, I. Iriepa, E. Galvez, J. Tamargo, E. Delpon, J. Pharmacol. Exp. Ther. 303 (2003) 862–873.
[13] K. Frenal, C.Q. Xu, N. Wolff, K. Wecker, G.B. Gurrola, S.Y. Zhu, C.W. Chi, L.D. Possani, J. Tytgat, M. Delepierre, Proteins 56 (2004) 367–375.
[14] M. Perry, M.J. de Groot, R. Helliwell, D. Leishman, M. Tristani-Firouzi, M.C. Sanguinetti, J. Mitcheson, Mol. Pharmacol. 66 (2004) 240–249.
[15] M. Perry, P.J. Stansfeld, J. Leaney, C. Wood, M.J. de Groot, D. Leishman, M.J. Sutcliffe, J.S. Mitcheson, Mol. Pharmacol. 69 (2006) 509–519.
[16] R.A. Pearlstein, R.J. Vaz, J. Kang, X.-L. Chen, M. Preobrazhenskaya, A.E. Shchekotikhin, A.M. Korolev, L.N. Lysenkova, O.V. Miroshnikova, J. Hendrix, D. Rampe, Bioorg. Med. Chem. Lett. 13 (2003) 1829–1835.
[17] H. Choe, K.H. Nah, S.N. Lee, H.S. Lee, H.S. Lee, S.H. Jo, C.H. Leem, Y.J. Jang, Biochem. Biophys. Res. Commun. 344 (2006) 72–78.
[18] R. Rajamani, B.A. Tounge, J. Li, C.H. Reynolds, Bioorg. Med. Chem. Lett. 15 (6) (2005) 1737–1741.
[19] Z. Zhou, V.R. Vorperian, Q. Gong, S. Zhang, C.T. January, J. Cardiovasc. Electrophysiol. 10 (1999) 836–843.
[20] W.J. Crumb Jr., Personal Communication, 9 August 2000.
[21] G.E. Kirsch, E.S. Trepakova, J.C. Brimecombe, S.S. Sidach, H.D. Erickson, M.C. Kochan, L.M. Shyjka, A.E. Lacerda, A.M. Brown, J. Pharmacol. Toxicol. Methods 50 (2004) 93–101.
[22] J. Wang, K. Della Penna, H. Wang, J. Karczewski, T.M. Connolly, K.S. Koblan, P.B. Bennett, J.J. Salata, Am. J. Physiol. Heart Circ. Physiol. 284 (1) (2003) H256–H267.
[23] S. Ekins, W.J. Crumb, R.D. Sarazan, J.H. Wikel, S.A. Wrighton, J. Pharmacol. Exp. Ther. 301 (2002) 427–434.
[24] Z. Zhou, Q. Gong, B. Ye, Z. Fan, J.C. Makielski, G.A. Robertson, C.T. January, Biophys. J. 74 (1) (1998) 230–241.
[25] A.A. Fossa, T. Wisialowski, E. Wolfgang, E. Wang, M. Avery, D.L. Raunig, B. Fermini, Eur. J. Pharmacol. 486 (2) (2004) 209–221.
[26] C. Davie, J. Pierre-Valentin, C. Pollard, N. Standen, J. Mitcheson, P. Alexander, B. Thong, J. Cardiovasc. Electrophysiol. 15 (11) (2004) 1302–1309.
[27] J.A. Yao, X. Du, D. Lu, R.L. Baker, E. Daharsh, P. Atterson, J. Pharmacol. Toxicol. Methods 52 (1) (2005) 146–153.
[28] P.J.S. Chiu, K.F. Marcoe, S.E. Bounds, C.-H. Lin, J.J. Feng, A. Lin, F.-C. Cheng, W.J. Crumb, R. Mitchell, J. Pharmacol. Sci. 95 (2004) 311–319.
[29] B. Drolet, S. Zhang, D. Deschenes, J. Rail, S. Nadeau, Z. Zhou, C.T. January, J. Turgeon, J. Cardiovasc. Electrophysiol. 10 (12) (1999) 1597–1604.
[30] D. Rampe, M.-L. Roy, A. Dennis, A.M. Brown, FEBS Lett. 417 (1997) 28–32.
[31] D. Rampe, M.K. Murawsky, J. Grau, E.W. Lewis, J. Pharmacol. Exp. Ther. 286 (1998) 788–793.
[32] D.J. Snyders, A. Chaudhary, Br. J. Pharmacol. 129 (2000) 893–900.
[33] S. Claassen, B.J. Zunkler, Pharmacology 74 (1) (2005) 31–36.
[34] B.R. Danielsson, K. Lansdell, L. Patmore, T. Tomson, Epilepsy Res. 55 (1–2) (2003) 147–157.
[35] A.A. Paul, H.J. Witchel, J.C. Hancox, Br. J. Pharmacol. 136 (5) (2002) 717–729.
[36] B.R. Danielsson, K. Lansdell, L. Patmore, T. Tomson, Epilepsy Res. 63 (1) (2005) 17–25.
[37] S. Ferreira, W.J. Crumb, C.G. Carlton, C.W. Clarkson, J. Pharmacol. Exp. Ther. 299 (2001) 220–226.
[38] R.D. Sarazan, W.J. Crumb Jr., C.M. Beasley Jr., J.T. Emmick, K.M. Ferguson, C.A. Strnat, P.J. Sausen, Eur. J. Pharmacol. 502 (3) (2004) 163–167.
[39] A.N. Katchman, K.A. McGroary, M.J. Kilborn, C.A. Kornick, P.L. Manfredi, R.L. Woosley, S.N. Ebert, J. Pharmacol. Exp. Ther. 303 (2) (2002) 688–694.
[40] L.M. Wu, M. Orikabe, Y. Hirano, S. Kawano, M. Hiraoka, J. Cardiovasc. Pharmacol. 42 (3) (2003) 410–418.
[41] A. Cavalli, E. Poluzzi, F. De Ponti, M. Recanatini, J. Med. Chem. 45 (2002) 3844–3853.
[42] A.M. Aronov, B.B. Goldman, Bioorg. Med. Chem. 12 (2004) 2307–2315.
[43] D.A. Doyle, J. Morais Cabral, R.A. Pfuetzner, A. Kuo, J.M. Gulbis, S.L. Cohen, B.T. Chait, R. MacKinnon, Science 280 (1998) 69–77.
[44] AMBER Version 8, University of California at San Francisco, San Francisco, CA, 2004.
[45] G.D. Hawkins, C.J. Cramer, D.G. Truhlar, Chem. Phys. Lett. 246 (1995) 122–129.
[46] G.D. Hawkins, J.J. Cramer, D.G. Truhlar, J. Phys. Chem. 100 (1996) 19824–19839.
[47] J.P. Ryckaert, G. Ciccotti, H.J.C. Berendsen, J. Comput. Phys. 23 (1977) 327–341.
[48] InsightII, Biosym/MSI, San Diego, CA, 1995.
[49] T.J.A. Ewing, I.D. Kuntz, J. Comput. Chem. 18 (1997) 1175–1189.